01,11

Short-range order in „disordered“ aluminum solid solutions in α-iron

© N.V. Ershov[1], N.M. Kleinerman[1], V.A. Lukshina[1], Yu.P. Chernenkov[3], D.A. Shishkin[1,2], O.P. Smirnov[3], V.G. Semenov[4]

[1] M.N. Mikheev Institute of Metal Physics, Ural Branch, Russian Academy of Sciences, Yekaterinburg, Russia
[2] Ural Federal University after the first President of Russia B.N. Yeltsin, Yekaterinburg, Russia
[3] St. Petersburg Nuclear Physics Institute, National Research Center Kurchatov Institute, Gatchina, Russia
[4] Insitute of Chemistry, Saint Petersburg University, St. Petersburg, Russia

E-mail: nershov@imp.uran.ru

Received: December 23, 2022
Revised: December 23, 2022
Accepted December 30, 2022

The atomic structure of soft magnetic iron-aluminum alloys is studied by X-ray diffraction and nuclear gamma-resonance spectroscopy. The concentration dependence of the body-centered cubic lattice constant and the short-range order (SRO) parameters in the region of a disordered solid solution is monitored. It is shown that in the concentration range from 3 to 18 at.% Al, the lattice constant increases almost linearly. Discrete decomposition of nuclear gamma resonance spectra makes it possible to determine such SRO parameters as the relative fractions of contributions from coordinations without Al atoms and with one, two, and three Al atoms in the first and second coordination shells. The deviation of the values of these fractions from the average statistical probabilities indicates the presence of a chemical order in the arrangement of atoms. The largest deviations are observed at 12 and 15 at.% Al. Conditions of preliminary heat treatment, such as quenching from the paramagnetic state and holding in the ferromagnetic state, give very similar values of the SRO parameters. The method is characterized by a high resolution in the hyperfine field, while having a rather high sensitivity for determining the intensity of individual contributions

Keywords: soft magnetic alloys, disordered Fe−Al solid solution, local ordering, X-ray diffraction, Mössbauer effect, distribution of atoms over coordination shells.

DOI: 10.21883/PSS.2023.03.55576.558

1. Introduction

Iron-rich alloys of iron and aluminum have attracted considerable scientific interest since 1932, when Bradley and Jay presented the results of X-ray diffraction studies of alloys of this system [1]. They showed that ordered phases with $B2$ and $D0_3$ structures are formed in the body-centered cubic (BCC) lattice of alloys containing more than ~ 19 at.% Al. In recent years, interest in Fe-Al alloys has increased again, since they exhibit high technological properties that are important for practical applications [2]. In addition, they can be used to study the critical behavior of a system upon phase transitions [3,4], for example, between ferromagnetic, paramagnetic, and spin-glasslike phases [5,6].

The phase diagram of the Fe-Al system has been refined many times over the years, but now there is a qualitative agreement between various studies of the nature of phases and order-disorder transitions in the Fe-rich regions of the diagram [7–16]. In the low-temperature part of the phase diagram [17,18] up to approximately 20 at.% Al, there is a region of α-phase (structure $A2$) or a substitutional disordered solid solution. Such alloys have soft magnetic properties and are characterized by features important for their practical application, which are associated with their structural state. These include induced magnetic anisotropy as an effect of thermomagnetic or thermomechanical treatment [19–23], a quadratic increase in the tetragonal magnetostriction coefficient with concentration [24,25] and behavior of electrical resistance versus temperature, unusual for most metals and alloys, the so-called „K-state“ [26,27].

Above 25 at.% aluminum, there are regions of α' and α'' phases with FeAl and Fe_3Al stoichiometry and $B2$ and $D0_3$ structures respectively [28]. Between 20 and 25 at.% two phases mix: above the temperature 550°C — phases α and α', and below — α and α''. A detailed description of the equilibrium phase diagram, the nature of transitions, and various potential mechanisms of phase transformations can be found in works [11,29].

With increasing aluminum concentration C_{Al}, the tetragonal magnetostriction coefficient λ_{100} of alloys in the α-zone of the phase diagram is characterized by a rapid increase proportional to C_{Al}^2 [30], and reaches a maximum at $C_{\mathrm{Al}}^2 = 0.17-0.19$. The course of the graph $\lambda_{100}(C_{\mathrm{Al}})$ up to 17 at.% Al does not depend, and after 17 at.% Al it depends on the cooling conditions of the alloy, which can be associated with the corresponding changes in their structural

state. Interestingly, if the alloy contains locally ordered pairs of aluminum atoms (for example, „Neel" pairs [31]), the number of which $N_{\mathrm{Al-Al}}$ is also proportional to C_{Al}^2, it turns out that at aluminum concentrations up to 17 at.%, the tetragonal magnetostriction coefficient is proportional to $N_{\mathrm{Al-Al}}$. Aluminum atoms in the BCC iron lattice replace iron atoms in an orderly manner rather than randomly, which ensures the growth of $\lambda_{100}(C_{\mathrm{Al}})$ at small values of C_{Al}.

A brief review of the previous results of structural studies of alloys of the iron-aluminum system in the α-region of the phase diagram, more precisely, at C_{Al} up to 25 at.% Al, was presented by us earlier [32], with the conclusion that above the Curie temperature (in the paramagnetic state) there is a tendency to the appearance of local ordering of the $B2$ type. At lower temperatures (in the ferromagnetic state), the short-range order of the $D0_3$ type is predominantly established. In the same paper, we present our original results of a study of short-range order in the arrangement of atoms in single crystals of an iron alloy with 7 at.% aluminum, obtained by means of diffuse X-ray scattering. It is shown that local ordering of atoms takes place in alloy samples. Clusters with an average size of 0.6−0.7 nm containing pairs of aluminum atoms, which are the second nearest neighbors, were found in the alloy, which fully corresponds to the predictions of the theory [33,34], which explains the dependences observed in the experiment electrical resistance and elastic properties of iron-rich alloys of iron-aluminum on concentration and temperature. The cluster has a structure of $B2$-type and consists mainly of two BCC cells with a common face, in the center of which are — aluminum atoms. Clusters $B2$ are characterized by axial shape anisotropy and are oriented equally probably along three crystallographic axes ⟨100⟩. Cells in clusters are deformed, aluminum and iron atoms are shifted from the nodes of an ideal lattice. The direction and magnitude of displacement of atoms were obtained earlier in ab initio calculations [35].

Anisotropic and deformed $B2$ clusters coexist with regions where local ordering of the $D0_3$ type occurs. The average size of these regions is approximately 0.6 nm, which corresponds to the parameter of one lattice cell $D0_3$. Since there are no noticeable shifts of the $D0_3$ diffuse peaks in $\theta-2\theta$-scans, we can assume that the displacements of atoms in the $D0_3$ cluster are small. $D0_3$ clusters with such characteristics were discovered for the first time due to the high sensitivity of the X-ray diffraction method [32]. The effect of heat treatment of alloy samples on the local ordering of atoms in them, in particular, annealing in the paramagnetic state followed by quenching in water and annealing in the ferromagnetic state [32], has been studied. Within the measurement accuracy, there is no difference in the local atomic ordering that occurs after such annealing. It turns out that not only the microstructure, but also the magnetic elastic properties of the alloy samples containing 7 at.% Al do not depend on their thermal history.

On the other hand, in the Fe-25% Al alloy, short-range $B2$ ordering of the FeAl type was found after quenching from 600°C, and deformation followed by slow cooling leads to the formation of the $D0_3$ of type Fe_3Al [36]. In addition, a new face-centered cubic phase of the $B1$ [37] type was discovered in the Fe-9% Al single crystal, in which the axes of the lattice cell of nanocrystals can be oriented relative to the axes of the BCC lattice. A similar phase $B1$ was observed earlier in Fe-Ga [38] alloys. Despite the available data, the physical reasons for the formation of the functional properties of Fe-Al alloys remain not fully understood and explained. The observed unusual phenomena are due to a change in the structure of the alloys. In the absence of long-range crystallographic order in alloys with a high concentration of iron (more than 82 at.%), a change in their properties can only be associated with a change in the nearest atomic neighborhood.

At present, the idea is being actively developed that local pair interactions of atoms of non-magnetic impurities in α-iron depend not only on the interatomic distance, but also on the nature of the ordering of the magnetic moments of iron atoms [39,40]. In the ferromagnetic state, at temperatures not exceeding the Curie point of the alloy, T_C, aluminum atoms at a distance of the first and second neighbors experience strong repulsion. The minimum interaction energy of the Al−Al pair is observed for the third and fourth neighbors, which leads mainly to the formation of a local order of the $D0_3$ type. Upon transition to the paramagnetic state ($T > T_C$), the disordering of the magnetic moments of iron atoms leads, on the one hand, to an increase in the energy of the Al−Al pair at a distance of the first neighbors, and on the other hand, to its decrease if the pair is in the position of the second neighbors [40]. The formation of locally ordered pairs of aluminum atoms of the $B2$ type becomes energetically favorable, therefore it is in the paramagnetic state that „Neel" Al−Al [31] pairs are formed.

The concentration and temperature dependence of the structure of single crystals of iron-silicon alloys with silicon concentrations from 0.06 to 0.10 [41] was studied by the neutron diffraction method. The intensities of superstructurel reflections, their ratios, as well as complex diffuse scattering profiles, were measured and analyzed. It was shown that at the lowest concentration of C_{Si}, up to a temperature of 600°C, the alloy can be considered as locally ordered, with the short-range order similar to $D0_3$. At $C_{\mathrm{Si}} \geq 0.076$, the diffraction patterns of all samples under normal conditions contain (100) and (1/2 1/2 1/2) reflections, which indicates to the long-range order of the phase $D0_3$; but as the temperature rises, the superstructure peaks gradually broaden and weaken. An analysis of diffuse scattering determines the temperature limit of the existence of the $D0_3$ phase at $C_{\mathrm{Si}} = 0.076$ as 500°C, and at $C_{\mathrm{Si}} = 0.09$ and 0.10 as 627°C. At a temperature of 800°C and above, no order is observed at all, which allows us to determine the temperature of 850°C as a disorder temperature, although, in accordance with the

phase diagram, the upper boundary of the phase zone $D0_3$ in Fe-Si alloys is at 700°C, which is slightly higher than the Curie temperature of the alloy. In binary alloys of the Fe-Al system, both the upper boundary of the $D0_3$ phase region and the Curie temperature are lower (approximately 670°C), so there is every reason to choose temperature 850°C as the disorder temperature, by analogy with alloys of the Fe-Si system.

Measurement and analysis of three-dimensional intensity distributions of diffuse scattering from single-crystal samples of iron-based alloys allows obtaining information on the short-range order in the arrangement of atoms, determining the type and size of zones with local ordering of [32,38,39]. At the same time, it has been repeatedly shown that the nuclear gamma-ray resonance (NGR) spectra of iron alloys are well described by subspectra, each of which corresponds to a specific configuration of iron atoms and impurities in the local surrounding of the iron atom [42–45]. Therefore, in structural studies, it is important to correctly group the contributions included in one of the main configurations $n_i = 0$, 1 and 2, where n_i — is the number of aluminum atoms in i-th coordination shell of the iron atom, and then analyze how the relative fractions of the main configurations change depending on the sample preparation conditions.

The purpose of this work is to study the concentration dependence of the short-range order parameters in the arrangement of atoms in iron-aluminum alloys in the region of a disordered solid solution of the phase diagram and the effect of heat treatments on it, such as quenching in water at room temperature after holding in the paramagnetic state and prolonged annealing in the ferromagnetic state. It is worth (1) to show the fundamental opportunity of determining the short-range order parameters in iron alloys with a small aluminum content via processing of the Mössbauer spectra; (2) determine the short-range order parameters in the region of a disordered solid solution and their dependence on aluminum concentration; (3) estimate the degree of deviation of the values of the short-range order parameters from the statistical average; (4) analyze the obtained results, interpret subtle features of the atomic structure of alloys; (5) evaluate the capabilities of the method, its place among other local methods for studying the atomic structure.

2. Experiment procedure

Ingots of iron-aluminum alloys with a content of 3, 6, 9, 12, 15 and 18 at.% Al were obtained by induction melting of Fe (99.95%) and Al (99.7%) in an argon atmosphere, from which plates approximately $10 \times 10\,\text{mm}^2$ in size and 0.24−0.64 mm thick were cut on an electric spark machine. For refining and removal of internal mechanical stresses, all samples were annealed (thermal annealing, TA) in a 10^{-5} mm Hg vacuum at a temperature of 1050°C for 4 h followed by a slow cooling with oven. After that, one sample of each composition was annealed in air for one hour at a temperature $T_{an} = 450$°C, which does not exceed the Curie temperature of the alloy (T_C decreases from 770 to 735°C as C_{Al} increases), and cooled slowly with oven. The second sample after a ten-minute annealing in air at a temperature $T_{an} = 850$°C in the paramagnetic state was quenched in water at room temperature (the quenching rate is approximately 400° C/s). Some of the samples were annealed in a previously evacuated and sealed ampoule at a temperature of 1050°C for 4 h, after which the ampoule with the sample was dropped into water at room temperature. The cooling rate is estimated as 350−400°C/s.

It is assumed that high-temperature holding should lead to disordering of impurity atoms in the BCC lattice of iron (or to ordering corresponding to the paramagnetic state), and quenching should fix this state. The annealing temperature of 450°C is significantly lower than the Curie point of the alloy, but is sufficient to activate the diffusion of aluminum in iron and achieve an equilibrium state during ferromagnetic ordering.

After heat treatments, the thickness of the samples was reduced by mechanical and chemical polishing to the optimum for X-ray diffraction and Mössbauer studies, up to 20 and 50 μm, respectively.

The Mössbauer spectra of resonant absorption were recorded using a CM1101 spectrometer in the constant acceleration mode. ^{57}Co in a metal matrix Rd served as the source of Mössbauer radiation. The number of channels per spectrum was 512.

To obtain information on the parameters of the hyperfine interaction at iron nuclei, the obtained Mössbauer spectra were fitted with subspectra using the SPECTR program included in the MSTOOLS [46] software package.

The results of the mathematical processing of the spectra are presented in the form of histograms of the distribution of the integral intensities of individual subspectra over hyperfine fields. The interpretation of the results is justified by the data on the dependence of the HFF on the number of aluminum atoms in the nearest coordination shells of the iron atom [43] and the results of the analysis of the spectra of disordered alloys α-FeSi [44,45].

3. Results and discussion

Previously, it was found [46] that as the concentration of aluminum increases from zero to ~ 20 at.%, i. e. in the region of a disordered substitutional solid solution, the BCC lattice cell parameter of the Fe-Al alloy increases monotonically. To observe a similar effect in our alloy samples containing 3−12 at.% aluminum, we measured the profiles of the main (Bragg) X-ray scattering peaks with indices (hkl), such as (110), (200), (211) and further up to (321) (according to the rule for the BCC lattice $h + k + l = 2m$, where m — is an integer). Then, the peak profiles were approximated by Gaussian functions, taking into account the background gradually decreasing with increasing scattering angle. Within the determination

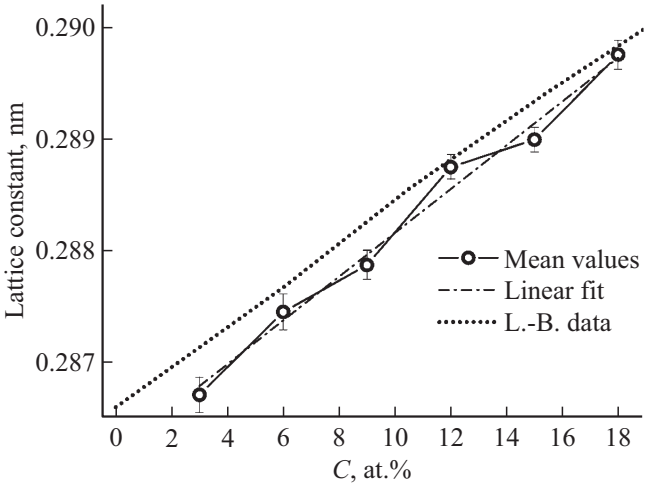

Figure 1. Concentration dependence of the BCC lattice constant $a(C)$ of the Fe-Al alloy in the concentration range from 3 to 18 at.% aluminum. L.-B. data from the database[46].

accuracy, the angular positions of the Bragg peaks and the calculated values of the cell parameter depend on the concentration, but do not depend on the heat treatment conditions. The positions of the maxima of identical Bragg peaks decrease with increasing C, where C — is the average aluminum concentration in the alloy, which corresponds to an increase in the lattice parameter a at Al concentrations from 3 to 18 at.%, as shown in Fig. 1, which shows the average values of the parameters $a(C)$ for alloys of the same composition.

The graph of $a(C)$ shown in Fig. 1 corresponds to the trend of increasing the BCC cell parameter with increasing aluminum concentration in our samples of Fe-Al alloys according to previously obtained data [46]. In this work, the content of the components was set in atomic percent, recalculated to the weight fractions of pure substances, which were then weighed and fused into an ingot. Samples were cut from ingots and subjected to heat treatments described in the previous section. When comparing experimentally determined unit-cell parameters $a(C)$, the accuracy of this determination (about $5 \cdot 10^{-4}$) should be taken into account. Comparison of the graphs shown in Fig. 1 shows that at two concentrations (12 and 18 at.% Al), the results are the same; at 6 at.%, there is practically no divergence of the dependences $a(C)$ as well. At two points (9 and 15 at.% Al), the obtained concentration is less than the predetermined one by approximately 1 at.% (which can be quite explained by experimental errors and is at the level of sensitivity of the dispersion method of scanning electron microscopy, which was used by us to control the value C), and only at the point 3 at.% the difference reaches 1 to 1.5 at.%. Since all the deviations of the $a(C)$ dependence for our samples from the data from the database [46] have the same sign (the concentrations do not exceed the predetermined values), this has a simple explanation: in the preparation and heat treatments, the samples lose more aluminum, light metal, more volatile at high temperatures, than iron. Nevertheless, in the further presentation of the results, we will use the concentration values given before melting to identify the alloys.

When iron atoms are replaced by more and more aluminum atoms in α-iron, the nuclear gamma resonance spectrum (NGR) broadens, as can be seen from a comparison of the spectra shown in Fig. 2. If at a concentration of 3 at.% Al the composite structure of the extreme peaks — the first and sixth is clearly observed, then at 6 and 9 at.% Al both the second and fifth peaks of the sextet take the same form. With an increase in the aluminum concentration to 18 at.%, the width of the lines increases several times, which is especially noticeable on the extreme lines of the sextet. The distribution of iron atoms over the values of the hyperfine field is discrete and depends on the specific local surrounding of the absorbing atom and the number of aluminum atoms in the first, second and third coordination shells. The observed changes in the experimental spectra are in full agreement with the results of the earlier analysis published in papers [22–24,29].

The broadening of the spectral lines is explained by the fact that in the spectrum, in addition to the coordination $n_1 = 0$, where n_i – is the number of aluminum atoms in the i-th coordination shell (CS) around an absorbing iron atom, configurations appear that include one, two or more ($n_1 = 1, 2, 3, \ldots$) impurity atoms in the first CS (the maximum number of atoms in the first CS is eight) [21,22]. The appearance of Al atoms in the first CS of an absorbing iron atom leads to a decrease in the hyperfine magnetic field (HMF) on its nucleus. As the aluminum content increases, both the number of coordinations, when $n_i \neq 0$, and the number of aluminum atoms in the first, second, and further CS increase. The NGR spectrum of the Fe-Al alloy is a superposition of individual subspectra, each of which corresponds to a configuration with a certain set of $n_1, n_2, n_3, \ldots$ [21,22]. As the distance from the resonant iron atom increases, the influence of impurity Al atoms decreases. The linewidths in the subspectra are approximately the same as in the spectrum of pure α-iron.

When one aluminum atom appears in the first CS, the HFF on the iron atom decreases by $\Delta H \approx 0.07 H_{\mathrm{Fe}}$ or approximately by 7%, where H_{Fe} — HFF value in pure α-hardware [21]; the decrease in HFF is proportional to the number of aluminum atoms in the first coordination sphere of the iron atom (n_1). For the most qualitative interpretation of the experimental NGR spectrum, it is required to take into account the contributions of the second and third spheres [22], and therefore the following coordinations can be distinguished: $(n_1\, n_2\, n_3) = (000), (010), (001), (011)$ included in $n_1 = 0$, $(n_1\, n_2) = (10), (11)$ and (12) in $n_1 = 1$ and $(n_1\, n_2) = (20)$ and (21) in $n_1 = 2$. In the work [22], the values of HFF shifts are established: $\Delta H \approx -7.0, -3.7, +1.3$ and -0.1% of HFe for one aluminum atom in the first, second, the third, and fourth CS, respectively.

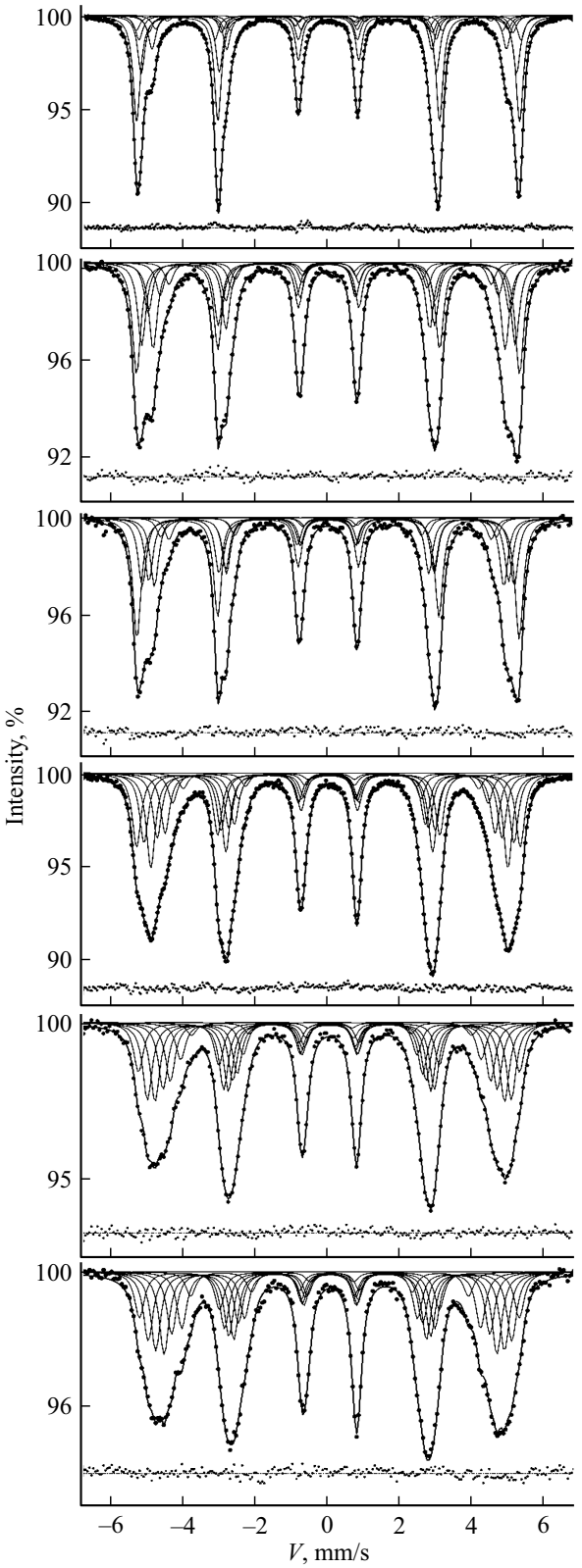

Figure 2. NGR spectra of Fe-Al alloy samples containing 3, 6, 9, 12, 15, 18 at.% aluminum quenched in water after holding in the paramagnetic state (shown by dots), and their fitting with subspectra (thin solid lines), sum of subspectra (solid line). The quality of the processing is shown by the differences between the experimental and calculated values of the total intensity of the subspectra below the spectra.

Theoretical and experimental studies of charge and spin perturbations near non-magnetic impurities in iron have confirmed [23,24] that the dependence of HMF shifts on the distance between Fe and Al atoms has an oscillating and rapidly decaying character. The NGR spectra of an alloy are well described by sums of subspectra, each of which corresponds to a certain configuration of iron atoms and impurities in the local environment of the iron atom [29]. It is important to correctly group the contributions included in one of the main configurations $n_1 = 0$, 1, 2 and 3, and then analyze how the relative fractions of the main configurations change depending on the sample preparation conditions. Previously, such a justification for the broadening of the NGR spectra of α-iron upon dissolution of non-magnetic impurities in it was successfully used for discrete analysis of the spectra of samples of iron-silicon alloys containing from 3 to 8 at.% silicon, after holding them at a temperature of 850°C and subsequent quenching in water and after annealing in the ferromagnetic state [44,45].

The NGR spectra measured on samples of iron-aluminum alloys containing from 3 to 18 at.% Al subjected to quenching are shown in Fig. 2. Figure 3 shows the spectra of samples containing 12–18 at.% Al. On the left — quenched in water after exposure in the paramagnetic state, on the right — annealed and slowly cooled in the ferromagnetic state. The spectra of samples of iron-aluminum alloys broaden significantly with increasing aluminum concentration (Fig. 2) and seem to be little (or almost independent) of the sample preparation conditions (Fig. 3). Since the initial NGR spectra of alloy samples containing the same amount of aluminum differ little depending on the heat treatment conditions, the spectra of all samples after all treatments are not given here. For demonstration, sets of only those spectra were selected that show concentration changes and comparisons of different heat treatments — quenching and annealing. It is shown that the spectra of samples of iron-aluminum alloys broaden significantly with increasing aluminum concentration and seem to be little dependent (or almost independent) of the sample preparation conditions

Using the SPECTR program of the MSTOOLS [47] package, mathematical simulation of each of the spectra was carried out, after fitting with subspectra, their sum was calculated — the result of fitting to the experimental spectrum and the discrepancy between the experimental and model spectra are also given in Fig. 2 and 3. When simulating the spectra, the number of subspectra was chosen to be minimal, sufficient for a qualitative description of the experimental distribution of the measured points of the spectrum. For all spectra, no more than eight subspectra were sufficient. Preliminary observations of the shape of the NGR spectra of samples of iron-aluminum alloys with a content of 3, 6, 9, 12, 15 and 18 at.% of aluminum, subjected to quenching and annealing, were reflected in the results of their discrete fitting in the form of histograms distribution of the intensity of absorption by iron atoms in terms of the magnitude of the hyperfine field — HMF, shown in Fig. 4 and 5.

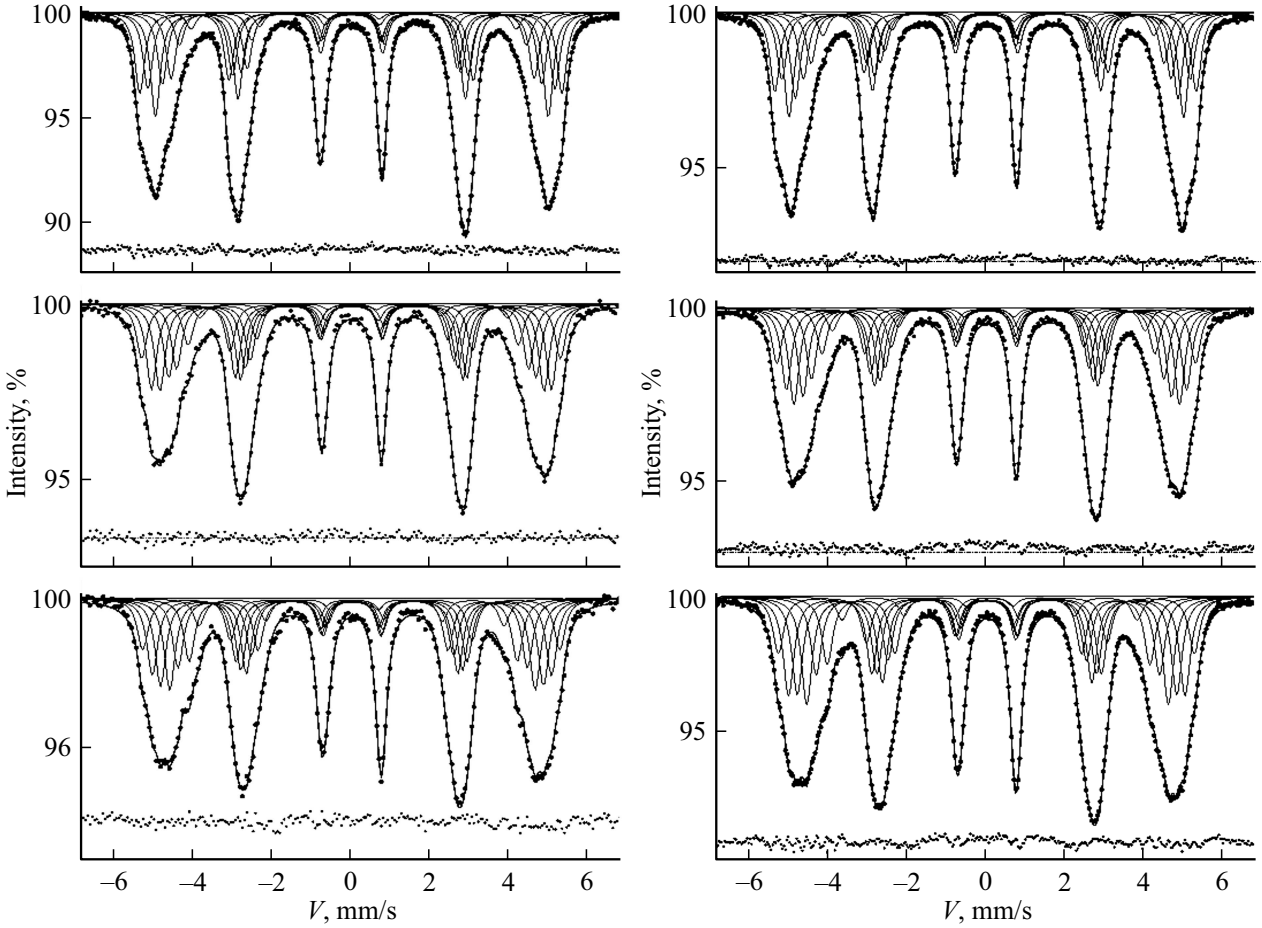

Figure 3. NGR spectra of iron-aluminum alloy samples containing 12, 15 and 18 at.% Al subjected to water quenching (left) and annealing (right).

As shown in Fig. 4, the main coordination 8:0 at the content of 3 at.% Al includes up to five lines, which, apparently, correspond to configurations with one or two Al atoms in the second and third CS. For example, (from left to right) $n_1n_2n_3 = 021, 020, 010, 000$ and 001. Let us remind that the presence of one Al atom in the second CS reduces the value of the HFF on the iron atom by about 4%, and in the third one — increases it by 1–2%. It is most probable that the two lines in coordination 7:1 correspond to the configurations $n_1n_2n_3 = 100$ and 111, since they have close HFF values. And coordination 6:2 consists of one line. If we continue to review Fig. 4, we see that for 6 at.% Al the coordination 8:0 contains only three lines (three separate configurations $n_1n_2n_3$): 020, 010 and 000. Coordination 7:1 has configurations $n_1n_2 = 12$, 11 and 10. In this case, the aluminum atom located in the first CS of the iron atom is the fourth neighbor of two in the case of $n_1n_2 = 12$ or one in the case of $n_1n_2 = 11$ to the aluminum atom of the second CS [44]. Coordination 6:2 contains one line, the contribution to which comes from all possible configurations with two Al atoms in the first CS of the iron atom. In the alloy with 9 at.% Al (Fig. 4) the coordination 8:0 contains configurations $n_1n_2n_3 = 020, 010$ and 000, coordination 7:1 — configurations 11 and 10, and coordination 6:2 — two configurations 20 and 21. In the last configuration, the aluminum atom from the second CS of the Fe atom is the fourth neighbor to both atoms of the first CS, and both Al atoms from the first CS belong to the same face of the BCC cell centered by the absorbing iron atom.

Exactly the same distribution of intensities along the HFF is observed in samples of the alloy containing 12 at.% Al, which is shown in Fig. 5. With an increase in the concentration to 15 at.% of aluminum, the intensity splitting in the 8:0 coordination simplifies to two lines. In this case, all coordinations consist of pairs of lines. In coordination 8:0 it is (from left to right) $n_1n_2 = 01$ and 00, in 7:1 — $n_1n_2 = 11$ and 10, in 6:2 — $n_1n_2 = 21$ and 20. For the first time, there is coordination contribution 5:3 represented by a single line. Similarly, coordination 8:0, 7:1 and 6:2 consist of pairs of lines, and there is a contribution of coordination 5:3 in the alloy at 18 at.% Al. As the concentration increases, the intensity of the lines corresponding to the contributions of aluminum atoms to the second CS of the iron atom increases. At 15 at.%, line 01 is more intense than line 00, and at 18 at.%, lines 01 and 11

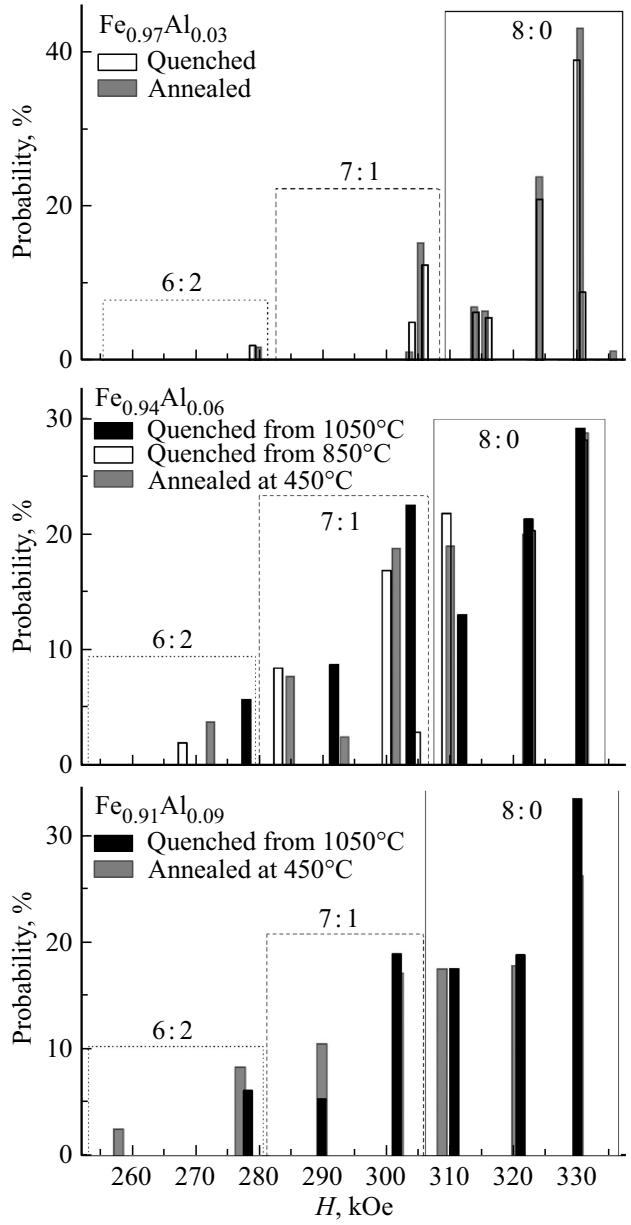

Figure 4. Histograms of intensities corresponding to the contributions of individual configurations around iron atoms, obtained by fitting the NGR spectra of iron-aluminum alloy samples containing 3, 6, and 9 at.% Al. Rectangles highlight the values of hyperfine fields (H, kOe), which we assigned to the coordinations 8:0 (solid line), 7:1 (dashed line) and 6:2 (dotted). The spectra of quenched samples are shown in Fig. 2.

are more intense than lines 00 and 10, respectively. The intensities I_4 corresponding to coordination 4:4, which may be a contribution from clusters or zones with $D0_3$ ordering, are not observed in all samples of alloys with aluminum concentrations from 3 to 18 at.%. The intensities of the main configurations are given in the table.

Aluminum concentrations and heat treatment temperatures of samples of Fe-Al alloys correspond to the zone of substitutional disordered solid solution (phase $A2$) [18]. At the same time, it is unlikely that the statistically average distribution of atoms over lattice sites will be realized, because at any concentration and under any conditions in alloys there are interatomic interactions that depend on the type of atom and on the distance between them. For instance, in Fe-Al alloys, strong repulsion prevents the formation of nearest neighbors of aluminum atoms, which is confirmed by both experimental and theoretical studies [48–50].

Experimentally observed intensities of the main configurations I_0 (coordination 8:0), I_1 (7:1) and I_2 (6:2) at most points are close to the statistically average probabilities,

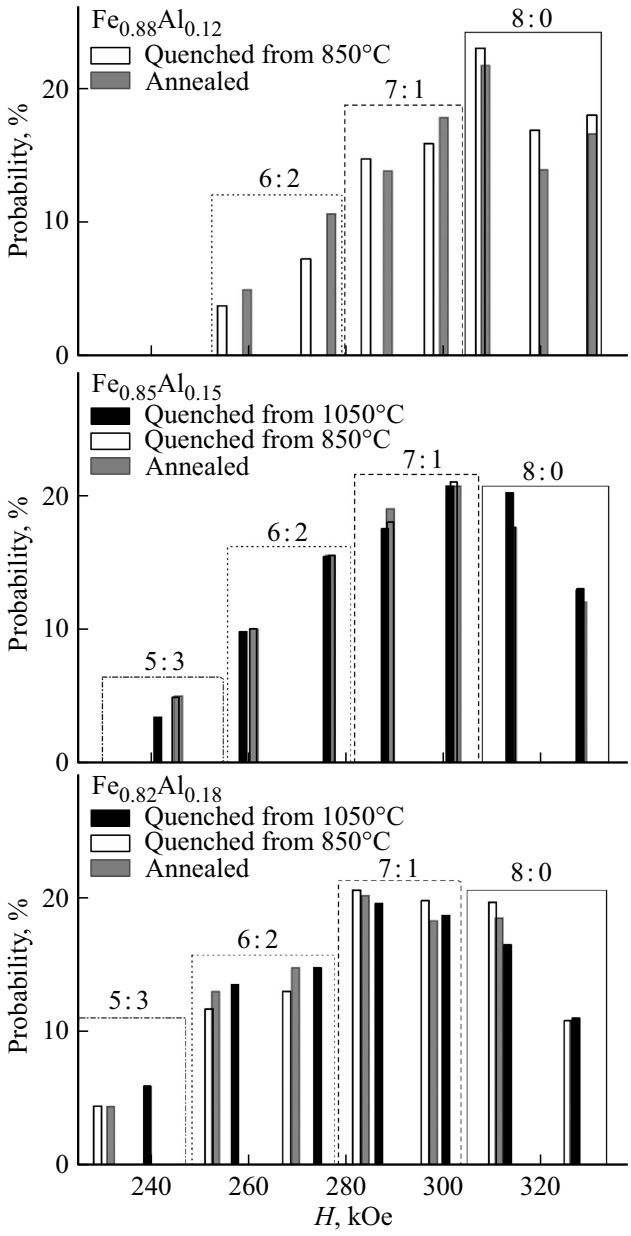

Figure 5. Histograms of intensities corresponding to the contributions of individual configurations around iron atoms, obtained by fitting the NGR spectra of iron-aluminum alloy samples given in Fig. 3.

The concentration dependence of the intensities of the main configurations in iron-aluminum alloys: in the case of a statistically average distribution of atoms over the sites of the BCC lattice (st.-av.) and in alloy samples subjected to heat treatment (quenching I (from 850°C), quenching II (from 1050°C) and annealing (450°C — 1 h))

at.% Al	TO	I_0 (8:0), %	I_1 (7:1), %	I_2 (6:2), %	I_3 (5:3), %	I_4 (4:4), %
3	st.-av.	78.4	19.4	2.1	–	–
	quenching I	81	17	2	–	–
	annealing	82	16	2	–	–
6	st.-av.	61.0	31.1	7.0	–	–
	quenching I	70	20	10	–	–
	quenching II	63	31	6	–	–
	annealing	67	29	4	–	–
9	st.-av.	47.0	37.2	12.9	2.5	–
	quenching II	70	24	6	–	–
	annealing	62	28	11	–	–
12	st.-av.	36.0	39.2	18.7	5.1	–
	quenching I	58	31	11	–	–
	annealing	52	32	16	–	–
15	st.-av.	27.2	38.5	23.8	8.4	1.8
	quenching I	30	39	26	5	–
	quenching II	33	38	25	3	–
	annealing	30	40	26	5	–
18	st.-av.	20.4	35.9	27.6	12.1	3.3
	quenching I	30	40	25	–	–
	quenching II	28	38	28	6	–
	annealing	29	38	28	4	–

which are shown in Fig. 6 by hollow circles connected by dash-dotted lines. However, this does not mean at all that in most cases, when iron is replaced by a small amount of aluminum in an alloy, a random distribution of atoms of two types over the sites of the BCC lattice is realized.

At the lowest concentration of aluminum, 3 at.%, the experimentally obtained intensities, firstly, do not depend on the conditions of heat treatment (quenching or annealing — in a hardened sample $I_0 = 81\%$, $I_1 = 17\%$ and $I_2 = 2\%$, and $I_0 = 82\%$, $I_1 = 16\%$, and $I_2 = 2\%$ in the annealed sample), and secondly, they are closest in value to the statistically average probabilities $I_0 = 81.7\%$, $I_1 = 16.8\%$, and $I_2 = 1.5\%$, which correspond to the binomial distribution of 2.5% of aluminum atoms in the BCC iron lattice. If we take into account the repulsion between aluminum atoms, then at first we can assume that the aluminum atoms are disordered so that they are neither first, nor second, nor third neighbors. Then there will be eight iron atoms (nearest neighbors) near one aluminum atom, the resonant absorption on which will contribute to 7:1 coordination in the NGR spectrum, which is equal to $8C$. For 3 at.% Al, this contribution to the I_1 intensity is 24%. At the same time, there should be no other coordinations with aluminum in the first CS, so the remaining 76% — is the intensity I_0 or the coordination contribution 8:0. Since the experimental intensities I_0 are greater, and I_1 are less than the average values, and, in addition, there is a small contribution I_2 in the experimental spectra, then the assumption of such isolation aluminum atoms is incorrect.

In the experimental intensities, there is a contribution from the coordination 6:2, the value of which is close to the statistically average value I_2. A completely isolated distribution of aluminum atoms is excluded, and two variants of the local distribution of atoms are possible: *1* — a random distribution (close to binomial), which is unlikely, and *2* — a small volume fraction of the order of the $B2$ type. If C_2 – is the concentration of aluminum atoms in $B2$ pairs, then their contribution to the coordination 7:1 will be $I_1 = 4C_2$, and contribution to 6:2 — $I_2 = 2C_2$. If all aluminum atoms at this concentration are in $B2$ pairs, then their contribution to $I_1 = 12\%$, and to $I_2 = 6\%$. In experimental spectra $I_2 = 2\%$. Therefore, approximately a third of the aluminum atoms ($C_2 \approx 1\%$) are in $B2$ pairs, and the fraction of aluminum atoms ($C_2 < C$) that make up the $B2$ pair is small. It turns out that it is impossible to uniquely determine the nature of the local ordering in the alloy at 3 at.% Al, although the second variant with $B2$ clusters is more preferable.

At aluminum concentrations of 6, 9 and 12 at.%, the experimental intensities I_0 and I_1 deviate from the statistical average. For coordination 6:2, the deviations of the intensity I_2 are insignificant and well within the limits of experimental errors. The largest deviations are at 9 and 12 at.% Al, and they clearly exceed the error value. If the experimental

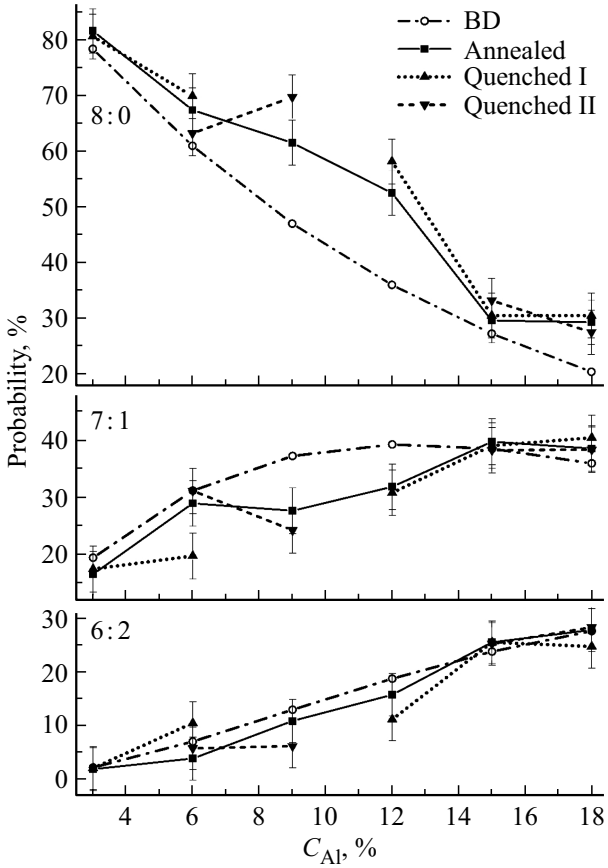

Figure 6. Concentration dependences of the intensities of contributions to the NGR spectra of configurations 8:0, 7:1 and 6:2. The graph compares the statistically average probabilities of configurations with configurations in alloy samples that have undergone different heat treatments. For the experimental values of the intensities, the range of potential errors is shown. Statistically average probabilities (BD — binomial distribution of atoms by CS) are shown on the graph by hollow circles, which are connected by dash-dotted lines.

intensities of I_0 coordination 8:0 are significantly higher than the corresponding statistically average probabilities, then the intensities I_1 of coordination 7:1, on the contrary, are lower. At the same time, both quenched and annealed samples have close values of the contribution intensities. Multidirectional deviations of the coordination intensities relative to the statistically average probabilities, namely: an excess for coordination 8:0 and a decrease for 7:1, indicate that the alloy is stratified into regions enriched in iron, which give an increased contribution to coordination 8:0, and enriched in aluminum, in which there is so much aluminum that they contribute to coordination with more than one number of atoms in the first CS of the iron atom.

Simulation of the distribution of atoms over the sites of the BCC lattice (software package DISCUS [50]) shows [51] that at a concentration C 6 at.% Al, aluminum atomic pairs $B2$ can be arranged in such a way that for each aluminum atom, out of six possible second neighbors, one will be an aluminum atom, the rest are iron atoms. In this case, the atoms of each $B2$ pair will be so isolated that they will not have aluminum atoms among the first and third neighbors. Atoms in $B2$ pairs are located along ⟨100⟩ axes, which in soft magnetic Fe-Al alloys are easy magnetization axes. A distinctive feature of this short-range order is the $4C$ contributions of iron atoms $I_1 = 24\%$ to the coordination 7:1, $2C$ of iron atoms $I_2 = 12$ % to coordination 6:2 and the ratio of these intensities $I_2/I_1 \approx 0.5$. The remaining Fe atoms are in the coordination 8:0, $I_0 = 64\%$. With a statistically average distribution of 6% Al, the intensities of individual coordinations: 8:0 ($I_0 = 61.0\%$), 7:1 ($I_1 = 31.1\%$) and 6:2 ($I_2 = 7.0\%$). In the experimental spectra of the alloy (6 at.% Al): after quenching $I_0 = 51\%$, $I_1 = 38\%$ and $I_2 = 10\%$; after annealing $I_0 = 67\%$, $I_1 = 29\%$ and $I_2 = 4\%$. The observed deviations (exceeding the error ±4%) both from the model of $B2$ pairs and from the statistically average distribution are explained by the fact that another local ordering is realized in the alloy.

Previously, by X-ray diffraction, we found that in the Fe-Al alloy containing 7−9 at.% aluminum, there are small zones ordered according to the $B2$ type ($B2$ clusters, including $B2$ pairs of Al−Al atoms), and phase clusters $D0_3$ with the size of one lattice cell $D0_3$ [32]. Therefore, it is required to analyze how these two types of local ordering manifest themselves in the NGR spectra of alloys. Consider the results for the alloy $Fe_{0.94}Al_{0.06}$ (6 at.% Al). In coordination 6:2, regardless of the heat treatment conditions, the analysis of the NGR spectra gives the intensities of the I_2 contributions (after quenching — 10%, after annealing — 4 %), close to the average (7%). After quenching, the intensity of coordination 7:1 ($I_1 = 38\%$) is higher than the average (31.1%), and coordination 8:0 ($I_0 = 51\%$) below the statistical average (61.0%), after annealing in the ferromagnetic state, the coordination intensity 8:0 ($I_0 = 67\%$) is slightly higher than the statistical average (61.0%), and the coordination 7:1 ($I_1 = 29\%$) is close to it. The increase in coordination intensity 8:0 after annealing is primarily due to the fact that the relative volume of the aluminum-depleted alloy increases compared to its average concentration, and, as a result, the relative volume of the aluminum-rich part increases. Most likely, local ordering develops in the latter. Al−Al pairs forming $B2$ clusters make the main contribution to the coordination 6:2 (I_2). If all aluminum atoms in this alloy were ordered into $B2$ pairs, then the I_2 intensity would have to approach 12%, and the contribution from the pairs to the I_1 intensity would be 24%.

But there are fewer aluminum atoms in $B2$ pairs, because after quenching $I_2 = 10\%$, and after annealing $I_2 = 4\%$. Simultaneously they contribute to the coordination 7:1 (after quenching $I_1 = 20\%$, after annealing $I_1 = 8\%$). If the total intensity I_1 after quenching is 38% and after annealing 29%, then the contribution to the coordination is 7:1 from individual aluminum atoms (8 Fe atoms each around one Al atom) or from $D0_3$ clusters (6 Fe atoms per Al atom in one $D0_3$ cluster) after heat treatment — 18 and 21%,

respectively. Let us note that the fractions of such atoms are practically independent of the heat treatment conditions. Thus, each individual Al atom specifies eight iron atoms in 7:1 coordination, and in the case of the $D0_3$ cluster, four Al atoms specify 24 Fe atoms in 7:1 coordination or six iron atoms per aluminum atom. The $D0_3$ clusters themselves should contribute to the coordination 4:4, when aluminum atoms are located in the neighborhood of one iron atom along the faces of the BCC cell, the connecting lines between which are — the diagonals of the faces. These aluminum atoms are each other's third neighbors. The remaining atoms of the first CS — are iron atoms. At a given concentration C, if all aluminum atoms participate in the formation of clusters $D0_3$, consisting of one cell $D0_3$, then the maximum fraction of the configuration 4:4 in the alloy cannot exceed $C/4 = 0.015$ ($I_4 \leq 1.5\%$), which is beyond the sensitivity of the NGR spectroscopy method. This is most likely why there is no 4:4 configuration in the spectra of the alloy containing 6 at.% aluminum.

The analysis showed that if after quenching in the alloy there is rather a large fraction of $B2$ pairs (~ 0.6 Al), fewer individual atoms (~ 0.3 Al) and even fewer cells $D0_3$, then after annealing, the fractions of $B2$ pairs and individual atoms decrease, whereas the fraction of cells $D0_3$ increases. Meanwhile, the fraction of $D0_3$ cells is not so large (small) to reach the sensitivity threshold of the NGR spectroscopy method ($I_4 \ll 4\%$).

Coordination 8:0 is formed mainly in the regions with low aluminum content. Fig. 6 shows a rather rapidly decreasing graph of the average values of I_0 with increasing Al concentration. Therefore, even slight deviations of the local aluminum concentration in small areas of the alloy from the average concentration lead to significant fluctuations in the coordination contribution 8:0 in the NGR spectrum. The experimental values of I_0 at 9 and 12 at.% Al correspond to the average statistical intensity values I_0 at 4–6% and 7–8%. The plots of the concentration dependence of the BCC lattice parameter shown in Fig. 1 demonstrate that such significant deviations from the average C_{Al} values are hardly possible. Individual aluminum atoms (if they do not have a second aluminum atom in the first, second and third CS) have 8 iron atoms in their first CS, which in the spectrum contribute only to the coordination 7:1 — I_1, the intensity of which, according to the experimental data at 9 and 12 at.% Al, is significantly less than the average statistical values.

The main types of local order (clusters $B2$ and $D0_3$), which are observed in the Fe-Al alloy, are characterized by the following. From each pair of Al atoms ordered according to the $B2$ type (two cells of the CsCl type joined by faces), there are two contributions to the NGR spectrum: I_1 (coordination 7:1) and I_2 (6:2) ($I_2/I_1 = 0.5$). Separate cells of the $D0_3$ phase, in which four aluminum atoms are located at the ends of the diagonals of the inner cube so that they are third neighbors to each other, contain 4 iron atoms that do not have an Al atom in the nearest neighborhood and give contribution to I_0 (8:0), 24 iron atoms, which have only one Al atom in their first CS (I_1, coordination 7:1), 6 iron atoms, which are located at the centers of the faces of the $D0_3$ cell, each have two Al atoms in their first CS (I_2, coordination 6:2). One iron atom that centers this cell has 4 Al atoms in the first CS (I_4, coordination 4:4).

Thus, it is possible to formulate the following regularities in the formation of NGR spectra of iron-aluminum alloys with an aluminum content in the region of a disordered solid solution. The NGR spectrum of an alloy consists of the sum of the subspectra of individual atomic configurations in the nearest neighborhood of an absorbing iron atom, realized in an alloy under certain conditions. The intensity of each of the subspectra corresponds to the relative volume fraction of a certain configuration in the alloy sample. The contribution to coordination 8:0 is given by: 1 — aluminum-depleted region of the $A2$ phase, 2 — individual clusters of the $D0_3$ phase (consisting of a single cell $D0_3$). One such cell contains 4 aluminum atoms and has 4 iron atoms in coordination 8:0. Therefore, if such cells contain C_3 of aluminum atoms, then their contribution to the coordination 8:0 or the intensity of I_0 is equal to C_3. The contribution to coordination 7:1 is given by: 1 — individual aluminum atoms (assume that the aluminum concentration in them is C_1), 2 — clusters of the $B2$ phase (the aluminum concentration is C_2) and 3 — cells of the $D0_3$ phase (aluminum concentration — C_3). Then $I_1 = 8C_1 + 4C_2 + 6C_3$. Further, the contribution to coordination 6:2 is given by: 1 — clusters of phase $B2$ (C_2) and 2 — cells of phase $D0_3$ (C_3). Then $I_2 = 2C_2 + 3/2C_3$. And obviously, $C = C_1 + C_2 + C_3$. There is no coordination 5:3 (I_3) for ideal phase clusters $B2$ and $D0_3$. But it may be formed in the process of an increase (growth) in the size of the regions of the $B2$ and $D0_3$ phases in intermediate states on defects in the atomic structure — for example, on vacancies or violations of the periodicity of the distribution of atoms over sites. In the ordered lattice of the $B2$ phase, all iron atoms have 8 aluminum atoms in the first CS (coordination 0:8) and 6 iron atoms in the second one ($n_1 n_2 = 80$). In the $D0_3$ phase lattice, there are two coordinations for iron atoms 8:0 ($n_1 n_2 = 06$) and 4:4 ($n_1 n_2 = 40$). It should be kept in mind that ordered superlattices can be formed only at stoichiometric compositions 25 and 50 at.% Al for the $D0_3$ and $B2$ phases, respectively.

Analysis of the NGR spectra of alloy samples containing 9 and 12 at.% Al, gives the same deviations for different heat treatments from the average values: the intensity of coordination 8:0 is higher, and coordination 7:1 — below the statistically average curve (Fig. 6), which corresponds to the bundle. Apparently, the relative volume of the alloy with a lower relative to the average aluminum concentration increases (intensity I_0 increases), while the aluminum concentration in regions with local ordering like $D0_3$ (increase the number of $B2$ pairs should lead to an increase in intensity I_2 (coordination 6:2)). But in the experimental spectra at 9 and 12 at.% Al, the intensity of this coordination after quenching is (6 and 11%) below the statistical average

(12.9 and 18.7%), and after annealing, within the error, it becomes (11 and 16% respectively) coinciding with the average. Unfortunately, for alloys containing 12, 15 and 18 at.% aluminum, we do not have the results of X-ray diffraction studies that could provide additional information on the nature of short-range ordering and the average sizes of regions with short-range order.

Obviously, at such concentrations of aluminum in alloys, there are no isolated aluminum atoms. The development of $D0_3$ phase regions in the limit can reach a volume fraction of 48% at $C = 12$ at.%, 60% at $C = 15$ at.% and 72% at $C = 18$ at.% Al. If the $D0_3$ phase coexists with isolated $B2$ pairs, then out of 12 at.% of Al atoms 4.1 at.% will be $B2$ pairs, the rest 7.9 at.% — areas of the $D0_3$ pair, which in volume fractions will be 68.3 and 31.7%, respectively. Pairs $B2$ will give contributions to the coordinations 7:1 ($I_1 = 16.4\%$) and 6:2 ($I_2 = 8.2\%$), and the phase zones $D0_3$ will contribute to the coordination 4:4 ($I_4 = 2\%$). In this case, I_4 is a very weak contribution, which can hardly be separated from the experimental spectrum. It turns out that if after quenching the intensity $I_1 = 31\%$ and $I_2 = 11\%$, and after annealing — $I_1 = 32\%$ and $I_2 = 16\%$, then a noticeable (45%) increase of I_2 while maintaining the value of I_1 is mainly due to the growing regions of the $D0_3$ phase, since an increase in the number of $B2$ pairs leads to an increase in the intensities of both I_2 and I_1. Meanwhile, the latter intensity increases twice as fast as the former.

At a concentration of 15 at.% Al, the volume fraction containing isolated clusters is $B2$ — 52.5%, and the volume fraction of phase zones $D0_3$ — 47.5%. At 18 at.% Al, the same volume fractions correlate as 36.8 and 63.2%. In the $Fe_{0.85}Al_{0.15}$ alloy samples, the distribution of intensities over coordinations (local order) is close to the statistically average and practically does not depend on the heat treatment conditions: quenching in water after holding at 850°C for 10 min, quenching after holding at 1050°C for 4 h or annealing in the ferromagnetic state at 450°C for 1 h. Similarly, the short-range order does not depend on the heat treatment conditions in the $Fe_{0.82}Al_{0.18}$ alloy samples, but in this case the measured intensities I_0 and I_1 slightly exceed the average, and the intensity of I_2 coincides with the average value I_2.

In all spectra of alloy samples with aluminum concentrations from 3 to 18 at.%, there are no I_4 intensities corresponding to 4:4 coordination, which can be a signal from the iron atom, centering the cell $D0_3$. But, starting from 15 at.% Al, the NGR spectra show coordination contributions 5:3 with values $I_3 = 3-5\%$ depending on processing at the average value of $I_3 = 8.4\%$. At 18 at.% Al $I_3 = 4-6\%$ (statistically average value $I_3 = 12.1\%$). Let us assume that at these concentrations (quite far from the stoichiometry of Fe_3Al) there is growth of regions ordered according to the $D0_3$ type, but they are characterized by a rather high defectiveness: either a large number of vacancies, or violations of the periodicity of the distribution of aluminum atoms over lattice sites $D0_3$.

For the appearance in the NGR spectrum of the contribution from coordination 4:4 or from four Al atoms in the first CS of the Fe atom, which is typical of the $D0_3$ phase, it is required that I_4 exceed 4%. Since there are 4 aluminum atoms per cell of the $D0_3$ phase, the maximum fraction of such cells in the alloy at an aluminum concentration C cannot exceed the value $C/4$, or $I_4 \leq 3.75\%$ for $C = 15$ at.% Al and $I_4 \leq 4.5\%$ for $C = 18$ at.% Al. Therefore, it turns out that the maximum possible contribution of the $D0_3$ phase to the NGR spectrum is on the edge of the sensitivity of the method. Within the region of the phase diagram corresponding to a disordered solid solution of aluminum atoms in the BCC iron lattice, aluminum atoms can be distributed over three possible zones: $A2$ disordered phase, $B2$ phase clusters, and regions with order $D0_3$. Therefore, the fraction of aluminum atoms in the $D0_3$ phase zones is only a part of their total number, and the contribution from the coordination 4:4 or from the $D0_3$ phase regions is not large enough to exceed the sensitivity limit of NGR spectroscopy ($\pm 4\%$).

4. Conclusion

Discrete fitting of the NGR spectra of alloys based on α-iron with a small aluminum content makes it possible to distinguish the contributions from both the main coordinations, such as 8:0, 7:1, 6:2 and 5:3, and from much finer configurations corresponding to different numbers of atoms in the second and third CSs of the absorbing iron atom. The method is characterized by a high resolution in the HFF, while having rather a high sensitivity in terms of the intensity of individual contributions.

The short-range order parameters — the intensity of the contributions of individual coordinations in the region of a disordered solid solution of 3−18 at.% aluminum in iron and their dependence on the aluminum concentration are determined. It is shown that the smallest deviations of the parameters from the statistical average (practically, i.e., taking into account the error in ±4%, they coincide) are observed at 3, 6 and 15, 18 at.% aluminum, and the largest — at 9 and 12 at.% of aluminum. Meanwhile, the intensities in the 8:0 coordination are higher than the average, and in the 7:1 coordination they are significantly lower, which is a sign of the local ordering of aluminum atoms in the α-Fe lattice. In addition, a significant effect of the conditions of heat treatment of alloy samples (quenching or annealing) on the nature of the local ordering of aluminum atoms was not found. If we compare this result with the behavior of the magnetostriction constant depending on the cooling conditions of the sample [30], then there is a contradiction that requires further special study. The effect on magnetostriction of the cooling rate of alloy samples with an aluminum content of more than 17 at.% shows that the effect is due to changes in the short-range atomic ordering, which were not detected in this study. Based on the analysis of results of the discrete fitting

of the NGR spectra, subtle features were found in the distribution of aluminum atoms along the CS around the iron atom. It was shown, for example, that in the main coordinations without Al atoms, with one and two Al atoms, the contributions without Al or with one Al atom to the second CS are also separated. Meanwhile, aluminum atoms are the fourth neighbors for each other.

The approach (method or technique) developed here is very promising for studying subtle features (changes) of short-range order in binary alloys of the Fe-Al system in the region of the *A*2 phase (disordered solid solution). Changes can occur as a result of various heat treatments, including in a magnetic field or in a field of mechanical stresses. The NGR spectroscopy method is quite sensitive to fairly small changes in the number of aluminum atoms in the first CS of the iron atom, and at the same time „sees" the atoms of the second sphere. At the same time, in order to increase the reliability of the results of the analysis of NGR spectra, it is useful to take information on the nature and size of the short-range order regions that can be realized in an iron-aluminum alloy.

Funding

The work was implemented as part of the state assignment of the Ministry of Education and Science of Russia (subject „Magnit", G.r. No. 122021000034-9), using the equipment of the CCU „Testing Center for Nanotechnologies and Advanced Materials" IPM Ural Branch of the Russian Academy of Sciences.

Conflict of interest

The authors declare that they have no conflict of interest.

References

[1] A.J. Bradley, A.H. Jay. Proc. R. Soc. London. Ser. A **136**, *829*, 210 (1932). https://doi.org/10.1098/rspa.1932.0075
[2] A.S. Freitas, D.F. de Albuquerque, I.P. Fittipaldi, N.O. Moreno. J. Magn. Magn. Mater. **362**, 226 (2014). https://doi.org/10.1016/j.jmmm.2014.03.055
[3] A. Oubelkacem, I. Essaoudi, A. Ainane, F. Dujardin, J. Ricardo de Sousa, M. Saber. Physica A **389**, *17*, 3427 (2010). https://doi.org/10.1016/j.physa.2010.04.033
[4] R.D. Shull, H. Okamoto, P.A. Beck. Solid State Commun. **20**, *9*, 863 (1976). https://doi.org/10.1016/0038-1098(76)91292-8
[5] S. Takahashi, X.G. Li, A. Chiba. J. Phys.: Condens. Matter **8**, *50*, 11243 (1996). http://iopscience.iop.org/article/10.1088/0953-8984/8/50/045/pdf
[6] S. Takahashi, H. Onodera, X.G. Li, S. Miura. J. Phys.: Condens. Matter **9**, *43*, 9235 (1997). DOI: 10.1088/0953-8984/9/43/009
[7] K. Oki, S. Towata, M. Tamiya, T. Eguchi. Trans. Jpn Inst. Met. **22**, *11*, 771 (1981). https://doi.org/10.2320/matertrans1960.22.771
[8] K. Oki, H. Sagane, T. Eguchi. Jpn J. Appl. Phys. **13**, *5*, 753 (1974). http://iopscience.iop.org/article/10.1143/JJAP.13.753/meta
[9] S.M. Allen, J.W. Cahn. Acta Met. **24**, *5*, 425 (1976). https://doi.org/10.1016/0001-6160(76)90063-8
[10] S.M. Allen, J.W. Cahn. Scripta Metallurg. Mater. **10**, *5*, 451 (1976). https://doi.org/10.1016/0036-9748(76)90171-X
[11] S.M. Allen. Phil. Mag. **36**, *1*, 181 (1977). DOI: 10.1080/00318087708244456
[12] W. Köster, T. Gödecke. Z. Metallkd. **71**, *12*, 765 (1980).
[13] K. Oki, A. Yamamura, M. Hasaka, T. Eguchi. Trans. Jpn Inst. Met. **18**, *7*, 520 (1977). https://doi.org/10.2320/matertrans1960.18.520
[14] M. Hasaka. Trans. Jpn Inst. Met. **21**, *10*, 660 (1980). https://doi.org/10.2320/matertrans1960.21.660
[15] H. Sagane, K. Oki, T. Eguchi. Trans. Jpn Inst. Met. **18**, *6*, 488 (1977). https://doi.org/10.2320/matertrans1960.18.488
[16] K. Oki, A. Yamamura, K. Kudo, T. Eguchi. T. Trans. Jpn. Inst. Met. **20**, *8*, 451 (1979). https://doi.org/10.2320/matertrans1960.20.451
[17] K. Han, I. Ohnuma, R. Kainuma. J. Alloys Comp. **668**, 97 (2016). https://doi.org/10.1016/j.jallcom.2016.01.215
[18] U.R. Kattner, B.P. Burton. Phase Diagrams of Binary Iron Alloys, Al-Fe. ASM International, Materials Park, OH (1993). P. 12. http://www.asminternational.org/documents/10192/1850140/57751G_Frontmatter.pdf/c36eeb4e-d6ec-4804-b319-e5b0600ea65d
[19] J. Steinert. Physica Status Solidi B **21**, *1*, K13 (1967). https://doi.org/10.1002/pssb.19670210149
[20] H. Wagner, H. Gengnagel. Physica Status Solidi B **9**, *1*, 45 (1965). https://doi.org/10.1002/pssb.19650090105
[21] M. Sugihara. J. Phys. Soc. Jpn **15**, *7*, 1456 (1960). http://dx.doi.org/10.1143/JPSJ.15.1456
[22] H.J. Birkenbeil, R.W. Cahn. J. Appl. Phys. **32**, *3*, S362 (1961). http://dx.doi.org/10.1063/1.2000470
[23] H.J. Birkenbeil, R.W. Cahn. Proc. Phys. Soc. **79**, *4*, 831 (1962). DOI: 10.1088/0370-1328/79/4/321
[24] J.B. Restorff, M. Wun-Fogle, K.B. Hathaway, A.E. Clark, T.A. Lograsso, G. Petculescu. J. Appl. Phys. **111**, *2*, 023905 (2012). https://doi.org/10.1063/1.3674318
[25] A.E. Clark, J.B. Restorff, M. Wun-Fogle, D. Wu, T.A. Lograsso. J. Appl. Phys. **103**, *7*, 07B310-1 (2008). https://doi.org/10.1063/1.2831360
[26] H. Thomas. Z. Metallkd. **41**, *6*, 185 (1950).
[27] H. Thomas. Z. Physik **129**, *2*, 219 (1951).
[28] R. Kuentzler. J. Physique **44**, *10*, 1167 (1983). https://hal.archives-ouvertes.fr/jpa-00209700
[29] S.M. Allen, J.W. Cahn. Acta Met. **23**, *9*, 1017 (1975). https://doi.org/10.1016/0001-6160(75)90106-6
[30] G. Bertotti, F. Fiorillo. In: Magnetic Alloys for Technical Applications. Soft Magnetic Alloys, Invar and Elinvar Alloys / Ed. H.P.J. Wijn. Springer-Verlag (1994). 7.1.2.3.3 Magnetostriction constants. P. 55–58. https://link.springer.com/chapter/10.1007/10065028_17 (limited access)
[31] I.B. Kekalo, B.A. Samarin. Fizicheskoye metallovedeniye pretsizionnykh splavov. Splavy s osobymi magnitnymi svoystvami. Metallurgiya, M., (1989). 496 p. (in Russian).
[32] N.V. Ershov, Yu.P. Chernenkov, V.A. Lukshina, O.P. Smirnov. FTT **60**, *9*, 1619 (2018). (in Russian). DOI: 10.21883/FTT.2018.09.46375.028 [N.V. Ershov, Yu.P. Chernenkov, V.A. Lukshina, O.P. Smirnov. Phys. Solid State **60**, *9*, 1661 (2018). DOI: 10.1134/S106378341809010X]
[33] F. Adunka, M. Zehetbauer, L. Trieb. Physica Status Solidi A **62**, *1*, 213 (1980). https://doi.org/10.1002/pssa.2210620124

[34] H.J. Leamy. Acta Metallurgica **15**, *12*, 1839 (1967).
[35] M.V. Petrik, Yu.N. Gornostyrev. Phys. Met. Metallogr. **114**, *6*, 469 (2013). DOI: 10.1134/S0031918X13060112
[36] V.I. Iveronova, A.I. Minaev, V.M. Silonov. FMM **33**, *5*, 978 (1972) (in Russian).
[37] Yu.P. Chernenkov, N.V. Ershov, V.A. Lukshina. Phys. Solid State **61**, *11*, 1960 (2019). DOI: 10.1134/S1063783419110118
[38] Yu.P. Chernenkov, N.V. Ershov, V.A. Lukshina. Phys. Solid State **60**, *12*, 2370 (2018). DOI: 10.1134/S1063783419010050
[39] O.I. Gorbatov, A.R. Kuznetsov, Y.N. Gornostyrev, N.V. Ershov, V.A. Lukshina, A.V. Ruban, Y.P. Chernenkov, V.I. Fedorov. JETP **112**, *5*, 848 (2011).
[40] O.I. Gorbatov, Yu.N. Gornostyrev, A.R. Kuznetsov, A.V. Ruban. Solid State Phenomena **172**–**174**, 618 (2011).
[41] K. Hilfrich, W. Kölker, W. Petry, O. Scharpf, E. Nembach. Acta Metallurg. Mater. **42**, *3*, 743 (1994).
[42] G.K. Wertheim. Mössbauer Effect: Principles and Applications. Academic Press Inc., N.Y. (1964).
[43] M.B. Stearns. Phys. Rev. B **6**, *9*, 3326 (1972).
[44] N.V. Ershov, N.M. Kleinerman, V.A. Lukshina, V.P. Pilyugin, V.V. Serikov. Phys. Solid State **51**, *6*, 1236 (2009).
[45] V.V. Serikov, N.M. Kleinerman, V.A. Lukshina, N.V. Ershov. Phys. Solid State **52**, *2*, 339 (2010).
[46] G. Bertotti, F. Fiorillo. In: Magnetic Alloys for Technical Applications. Soft Magnetic Alloys, Invar and Elinvar Alloys / Ed. H.P.J. Wijn. Springer-Verlag (1994). 7.1.2.2.1 Phase diagrams, lattice parameters and density, thermal expansion. P. 42. https://materials.springer.com/lb/docs/sm_lb_978-3-540-47246-9_11
[47] B.C. Rusakov. Mössbauer spectroscopy of locally heterogeneous systems. CCNSR INP NNC RK, Almaty (2000). 438 p. (in Russian).
[48] V. Pierron-Bohnes, M.C. Cadeville, A. Finel, R. Caudron, F. Solal. Physica B: Condens. Matter **180**–**181**, *2*, 811 (1992).
[49] V. Pierron-Bohnes, S. Lefebvre, M. Bessiere, A. Finel. Acta Metallurg. Mater. **38**, *12*, 2701 (1990). https://doi.org/10.1016/0956-7151(90)90284-N
[50] M.V. Petrik, Y.N. Gornostyrev. Phys. Met. Metallogr. **114**, *6*, 469 (2013).
[50] Th. Proffen, R.B. Neder. J. Appl. Crystallography **30**, *2*, 171 (1997).
[51] Yu.P. Chernenkov, N.V. Ershov, V.A. Lukshina, V.I. Fedorov, B.K. Sokolov. Physica B: Condens. Matter **396**, *1–2*, 220 (2007).

Translated by E.Potapova